articles

molecular pharmaceutics

Study of the Amorphous Glibenclamide Drug: Analysis of the Molecular Dynamics of Quenched and Cryomilled Material

Z. Wojnarowska,* K. Grzybowska, K. Adrjanowicz, K. Kaminski, M. Paluch, L. Hawelek, R. Wrzalik, and M. Dulski

Institute of Physics, University of Silesia, ul. Uniwersytecka 4, 40-007 Katowice, Poland

W. Sawicki

Department of Pharmaceutical Technology, Medical University of Gdansk, Hallera 107, 80-416, Gdansk, Poland

J. Mazgalski and A. Tukalska

Preformulation Department R&D, Pharmaceutical Works Polpharma SA, Pelplinska 19, 83-200 Starogard Gdanski, Poland

T. Bieg

Silesian University of Technology, Department of Chemistry, Division of Organic Chemistry, Biochemistry and Biotechnology, ul. Krzywoustego 4, 44-100 Gliwice, Poland

Received March 21, 2010; Revised Manuscript Received June 29, 2010; Accepted July 15, 2010

Abstract: Glibenclamide (GCM) is an oral hypoglycemic agent of the sulfonylurea group used in the treatment of non-insulin-dependent diabetes. Crystalline GCM is characterized by low bioavailability, which is attributed to its poor dissolution properties. It prompted us to prepare this drug in its amorphous form as a means to enhance its dissolution characteristics. Two different methods were used to convert crystalline GCM into the glassy form: quench-cooling of the melt and cryogenic milling. To monitor solid-state properties of the amorphous samples, X-ray powder diffraction (XRD), infrared spectroscopy (FT-IR), differential scanning calorimetry (DSC), ultraperformance liquid chromatography (UPLC) and spectroscopy, and broadband dielectric spectroscopy (BDS) were applied. The results of UPLC separations along with associated infrared and NMR measurements unambiguously showed that the thermal degradation of the quenched GCM, as suggested in literature reports, does not occur. A similar analysis performed on the cryomilled material also did not indicate any chemical decomposition. On the other hand, both methods confirmed that the conversion to the amorphous form is connected with the amide−imidic acid tautomerism of the examined drug. Moreover it was shown that this transformation occurs regardless of the manner of amorphization. Finally, dielectric spectroscopy was employed to study the molecular dynamics of vitrified GCM. The analysis of the $\varepsilon''(f)$ in terms of the KWW function from the dielectric measurements revealed the existence of an "excess wing" attributed to the true Johari−Goldstein process based on Ngai's coupling model. The dielectric properties of GCM obtained in the amorphous form both by rapid cooling of the melt and the cryogenic grinding of crystalline sample were also compared.

Keywords: Glibenclamide; cryogrinding; molecular dynamics; amide-imidic acid tautomerism; thermal decomposition

10.1021/mp100077c
Published on Web 07/16/2010

Introduction

Glibenclamide (GCM) is one of the most prescribed oral pharmaceuticals used to treat type II of diabetes mellitus (non-insulin-dependent diabetes mellitus, NIDDM).[1] This antidiabetes drug stimulates the pancreas to produce and release insulin which regulates the blood sugar level. It also encourages sugar in the blood to travel to cells where it is needed to be converted into energy. Because of its low aqueous solubility (~38 μmol/L at 37 °C)[2] and poor dissolution rate, GCM has been classified as a class II compound in the Biopharmaceutical Classification System (BCS).[3] In order to improve the solubility of GCM, several formulation strategies such as micronization,[4] molecular dispersion,[5] incorporation of surfactants,[6] complexation with cyclodextrin[7] and glass formation[8,9] have been reported in the past. The last method from the preceding list is very widely applied to enhance the rate of dissolution and thus to promote the therapeutic activity of pharmaceutical materials. In the literature, one can find many examples showing that active pharmaceutical ingredients (APIs) prepared in the amorphous state are markedly more soluble and consequently have better bioavailability than their crystalline counterparts.[10,11] In addition, a better facility to form tablets from such crystalline counterparts has also been also reported.[12]

For the preparation of pharmaceutical systems in their amorphous form, generally, four established ways are known: (1) condensation from the vapor state, (2) supercooling of the melt, (3) mechanical activation of a crystalline mass (e.g., during milling), and (4) rapid precipitation from solution (e.g., during freeze-drying or spray drying).[13] The simplest method among them is based on the rapid cooling of the molten sample of a pharmaceutical system. However, the method becomes ineffective if chemical degradation occurs during the melting of crystal. The high thermal stress accompanying melting can be reduced, for example by ball milling; but the free excess enthalpy induced by mechanical activation has been also shown to accelerate chemical degradation of the sample.[14] In the recent past, cryogenic grinding (also known as cryogenic mechanical milling, CMM), as an alternative to room temperature milling, has attracted much attention. This method is much more efficient than ball milling to prepare glassy drugs as it is believed that chemical degradation does not occur in this case. Thus, there has been no literature precedence demonstrating that CMM causes the decomposition of cryomilled samples. However, it has been reported that the ground material has a lower stability than the quenched one.[15]

The first amorphization of GCM by melting and quench cooling was carried out in 1991 by Hassan et al.[8] They observed that the rapid cooling of the melt resulted in an amorphous compound with solubility 10 times higher than the crystalline form. Moreover, they found that the GCM drug exhibited keto−enol tautomerism. This suggested that a GCM molecule existed in equilibrium with its two easily interconvertible constitutional isomers (see Figure 1). This phenomenon was also observed by other researchers studying GCM.[8,16−18] It was repeatedly reported that the transition from a predominantly keto to a predominantly enol form occurs when GCM is converted to its amorphous form.

* Corresponding author. Mailing address: University of Silesia, Institute of Physics, ul. Uniwersytecka 4, 40-007 Katowice, Poland. E-mail: zwojnaro@us.edu.pl. Tel: (+48) 32 359 1323. Fax: (+48) 32 258 84 31.

(1) Mutalik, S.; Udupa, N. Glibenclamide Transdermal Patches: Physicochemical, Pharmacodynamic, and Pharmacokinetic Evaluations. *J. Pharm. Sci.* **2004**, *93* (4), 1577.
(2) Hartke, K., Ed. *Comments to the European Pharmacopoeia*, 14th ed.; WVG mbH: Stuttgart, 2001.
(3) Dressman, J.; Butler, J.; Hempenstall, J.; Reppas, C. *Pharm. Technol.* **2001**, *7*, 68.
(4) Rupp, W.; Badian, M.; Heptner, W.; Malerczyk, V. Bioavailability and in vitro liberation of glibenclamide from a new dosage form. *Biopharm. Pharmacokinet., Eur. Congr., 2nd* **1984**, *1*, 413–420.
(5) Ganley, J. A.; McEven, J.; Calvert, R. T.; Barker, C. J. The effect of in vivo dispension and gastric emptying on glibenclamide absorption from a novel, rapidly dissolving capsule formulation. *J. Pharm. Pharmacol.* **1984**, *36*, 734–739.
(6) Singh, J. Effect of sodium lauryl sulfate and Tween® 80 on the therapeutic efficacy of glibenclamide tablet formulations in terms of BSL lowering in rabbits and diabetic human volunteers. *Drug Dev. Ind. Pharm.* **1986**, *12*, 851–866.
(7) Mitrevej, A.; Sinchaipanid, N.; Junyaprasert, V.; Warintornuwat, L. Effect of grinding of β-cyclodextrin and glibenclamide on tablet properties. *Drug Dev. Ind. Pharm.* **1996**, *22*, 1237–1241.
(8) Hassan, M. A.; Najib, N. M.; Suleiman, M. S. Characterization of glibenclamide glassy state. *Int. J. Pharm.* **1991**, *67*, 131–137.
(9) Salem, M. S.; Najib, N. M.; Hassan, M. A.; Suleiman, M. S. Dissolution kinetics of glibenclamide glass. *Acta Pharm. Hung.* **1997**, *67*, 13–17.
(10) Hancock, B. C.; Parks, M. What is the True Solubility Advantage for Amorphous Pharmaceuticals? *Pharm. Res.* **2000**, *17* (4), 397–404.
(11) Hancock, B. C.; Zografi, G. Characteristics and significance of the amorphous state in pharmaceutical systems. *J. Pharm. Sci.* **1997**, *86*, 1–12.
(12) Kaminski, K.; Kaminska, E.; Adrjanowicz, K.; Grzybowiska, K.; Wlodarczyk, P.; Paluch, M.; Burian, A.; Ziolo, J.; Lepek, P.; Mazgalski, J.; Sawicki, W. Dielectric relaxation studies on tramadol and its hydrochloride salt. *J. Pharm. Sci.* **2009**, *99*, 94–106, 1.
(13) Bruno, C.; Hancock, B.; Zografi, G. Characteristics and Significance of the Amorphous State in Pharmaceutical Systems. *J. Pharm. Sci.* **1997**, *86*, 1.
(14) Huttenrauch, R.; Fricke, R.; Zielke, P. Mechanical activation of pharmaceutical systems. *Pharm. Res.* **1985**, *2*, 302–306.
(15) Crowley, J. K.; Zografi, G. Cryogenic grinding of indomethacin polymorphs and solvates: Assesment of amorphous chase formation and amorphous chase physical stability. *J. Pharm. Sci.* **2001**, *91* (2), 492.
(16) Panagopoulou-Kaplani, A.; Malamataris, S. Preparation and characterization of new insoluble polymorphic form of glibenclamide. *Int. J. Pharm.* **2000**, *195*, 239.
(17) Patterson, J. E.; James, B. M. B.; Forster, A. H.; Lancaster, R. W.; Butler, J. M.; Rades, T. The Influence of Thermal and Mechanical Preparative Techniques on the Amorphous State of Four Poorly Soluble Compounds. *J. Pharm. Sci.* **2005**, *94* (9), 1999.

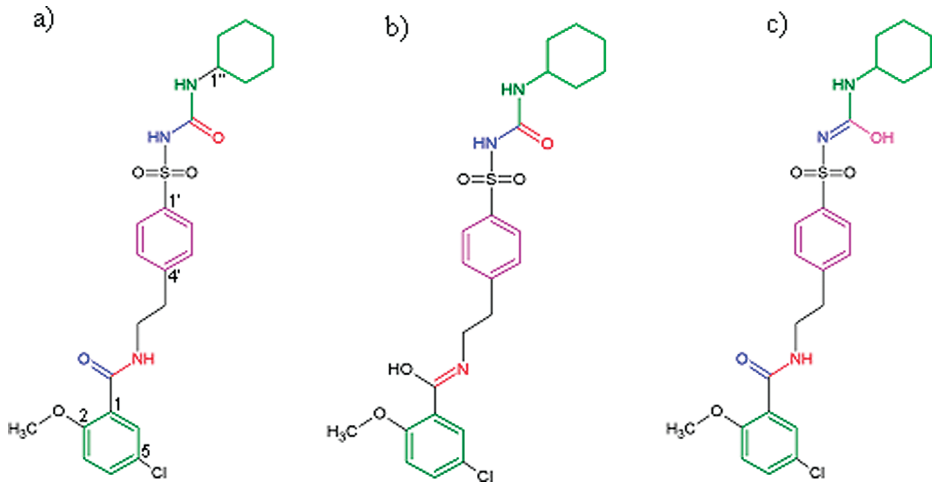

Figure 1. The chemical structure of glibenclamide drug. Panel (a) presents the molecule in the amide form while on panels (b) and (c) the possible imide forms of GCM are depicted.

Moreover, it has also been established that the tautomerism occurs regardless of the amorphization method used.

Equally importantly, Hassan et al. also reported that the molecular decomposition of GCM does not occur during the melting process. Based on this, Panagopoulou-Kapalani and Malamataris[16] annealed a GCM sample at 458 K for 5 min, to ensure a complete melting of the sample, which was subsequently cooled in two different ways, at a slower rate and a rapid rate. Similarly to Hassan et al., Panagopoulou-Kapalani and Malamataris also did not observe the decomposition of GCM in spite of the fact that the sample was held for a sufficient time at a temperature higher than its melting point. Moreover, they found that the quick cooling of the molten GCM led to a new crystalline arrangement that melted at 315 K, which is lower than the melting temperature of the commercial GCM drug ($T_m = 440$ K). In addition, the solubility of this new form was 20 times higher than that of the commercial GCM drug.[16] In light of this previous data, a very recent report by Patterson et al.[17] on the stability of GCM is a contradiction as it was reported that the melting and quench cooling of a GCM sample results in an unacceptably high degree of chemical degradation. These contradictory literature reports have prompted us to conduct a comprehensive analysis on GCM that we expect will answer the following question: *Does the decomposition of glibenclamide drug occur during melting?* Based on such an analysis, a detailed study of the structure, molecular dynamics and the tendency for crystallization of GCM drug is presented below.

In addition, in this work, we have chosen to use two different sample preparation techniques, namely, the quench cooling of the melt and the cryogrinding of the sample, to obtain the GCM drug in the amorphous form. The produced amorphous samples were subsequently analyzed with the use of several measurement techniques such as X-ray powder diffraction (XRD), Fourier transform infrared spectroscopy (FT-IR), differential scanning calorimetry (DSC), ultraperformance liquid chromatography (UPLC) and broadband dielectric spectroscopy (BDS). Prior to this study, the last two methods had not been previously applied to characterize the GCM drug. UPLC, one of the most sensitive analytical methods, and associated FT-IR measurements were used to clarify the contradictions in the literature reports on the thermal degradation of GCM. Furthermore, dielectric spectroscopy, which is often applied to study liquid−glass transitions in various pharmaceuticals,[12,19−21] was employed to characterize the molecular dynamics of GCM. Finally, we also examine the crystallization properties of amorphous GCM.

Experimental Section

Material. The tested GCM drug (5-chloro-*N*-[2-[4-(cyclohexylcarbamoylsulfamoyl)phenyl]ethyl]-2-methoxybenzamide ($C_{23}H_{28}ClN_3O_5S$) MW = 493.14 g/mol) was supplied from Polpharma Pharmaceutical Works Poland as a white crystalline powder and had a chemical purity of greater than 99.5%, as determined by UPLC analysis. The X-ray diffractogram of GCM revealed a completely crystalline form of the drug (see black line in Figure 2) in agreement with Panagopoulou-Kapalani and Malamataris. The authors had

(18) Fukami, T.; Furuishi, T.; Suzuki, T.; Hidaka, S.; Ueda, H.; Tomato, K. Improvement of solubility of polory water soluble drug by cogrinding with highly branched cyclic dextrin. *J. Inclusion Phenom. Macrocyclic Chem.* **2006**, *56*, 61–64.

(19) Bras, A. R.; Noronha, J. P.; Antunes, A. M. M.; Cardoso, M. M.; Schonhals, A.; Affouard, F.; Dionisio, M.; Correia, N. T. Molecular motions in amorphous Ibuprofen as studied by Broadband Dielectric Spectroscopy. *J. Phys. Chem. B* **2008**, *112* (35), 11087–11099.

(20) Adrjanowicz, K.; Kaminski, K.; Paluch, M.; Wlodarczyk, P.; Grzybowska, K.; Wojnarowska, Z.; Hawelek, L.; Sawicki, W.; Lepek, P.; Lunio, R. Dielectric Relaxation Studies and Dissolution Behavior of Amorphous Verapamil Hydrochloride. *J. Pharm. Sci.* **2010**, *99* (2), 828–839.

(21) Adrjanowicz, K.; Wojnarowska, Z.; Wlodarczyk, P.; Kaminski, K.; Paluch, M.; Mazgalski, J. Molecular mobility in liquid and glassy states of Telmisartan (TEL) studied by Broadband Dielectric Spectroscopy. *Eur. J. Pharm. Sci.* **2009**, *38* (5), 395–404.

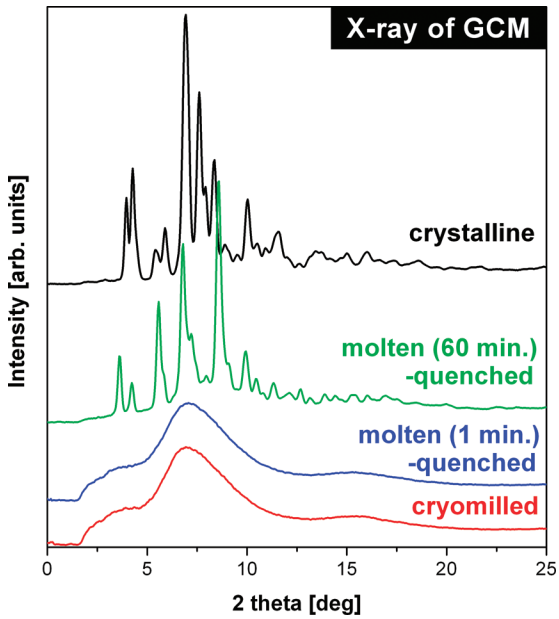

Figure 2. X-ray powder diffraction patterns of glibenclamide: (a) crystalline, (b) heated at the melting point for 60 min and then quenched, (c) molten for 1 min and next quick quenched, (d) obtained by cryogenic grinding (top to bottom).

also presented the X-ray diffraction patterns for the new polymorphic form of GCM. Since there were extensive differences in the intensities and positions of the Bragg peaks between the raw material and the new crystalline form of GCM, we could easily identify that the crystalline structure of our tested GCM sample is the same as the structure of the GCM material studied by Panagopoulou-Kapalani and Malamataris. The sample was used without any further purification.

Methods

Preparative Techniques. Quench-Cooling of the Melt. The crystalline GCM drug was placed on a stainless steel plate and was heated on a hotplate until a complete melt was achieved (as determined by visual inspection). In a subsequent step, the sample was quickly quenched by putting onto a cold tile.

Cryogenic Grinding of the Crystalline GCM. Cryogenic grinding of GCM was carried out by means of a 6770 SPEX freezer/mill. In order to ensure that the examined sample was anhydrous, it was dried at 353 K in a vacuum oven for 16 h. The total mass of the milled GCM was 1 g. The sample was placed in a stainless steel vessel and was immersed in liquid nitrogen. Placed in the vessel stainless steel rod, it is vibrated by means of magnetic coil. Prior to the start of grinding, the sample was subjected to 10 min of precooling. The mill was set to function at an impact frequency of 15 Hz for 6 min grinding intervals that were separated by 3 min each of cool-down periods. The total grinding time was 3 h. After such a detailed grinding procedure, one can be certain that the amorphization of GCM proceeds to completion. After the cryogenic grinding, the vessel with the ground sample was placed in a vacuum oven and was allowed to warm to room temperature. The prepared ground GCM sample was subsequently analyzed by the following analytical methods.

Analytical Techniques. XRD Measurements. XRD experiments were performed at ambient temperature on Rigaku-Denki D/MAX RAPID II-R diffractometer (Rigaku Corporation, Tokyo, Japan) with a rotating anode Ag Kα tube (λ = 0.5608 Å), an incident beam (002) graphite monochromator and an image plate in the Debye−Scherrer geometry. The pixel size was 100 mm ×100 mm. Studied samples were placed inside Lindemann glass capillaries (1.5 mm in diameter). Then, the measurements were performed on sample-filled and empty capillaries and the intensity for the empty capillary was subtracted. The beam width at the sample was 0.1 mm. The two-dimensional diffraction patterns were converted into one-dimensional intensity data using a suitable software.

Ultraperformance Liquid Chromatography (UPLC) Measurements. The ACQUITY UPLC system utilized for the measurements consisted of a binary solvent manager, sample manager, column manager, photodiode array eλ detector and a computer with installed Empower software for UPLC controlling and data processing (Waters, Millford, MA). The UV detector wavelength was set at 230 nm. Separation was achieved using an ACQUITY UPLC C18 column (1.7 μm, 2.1 mm ×50 mm, Waters, Wexford, Ireland). The mobile phase consisted of acetonitrile (mobile phase A) and 0.1% (v/v) triethylamine and was adjusted to a pH of 3.0 with ortho-phosphoric acid (mobile phase B). The program ran at 50% of mobile phase A and 50% of mobile phase B at a flow rate of 0.25 mL/min. The sample solvent was a mixture of acetonitrile and water (80:20, v/v). All of the presented UPLC chromatograms have been obtained by subtracting the peak belonging to the acetonitrile solvent (t_R = 0.49 min).

Differential Scanning Calorimetry (DSC) Measurements. DSC measurements of GCM were carried out using a Perkin-Elmer Pyris 1 DSC instrument utilizing cooling by liquid nitrogen. The samples were analyzed under helium purge (20 mL/min) in hermetically sealed aluminum pans. The instrument was calibrated for temperature and heat flow using high-purity standards of indium. The thermal analysis was carried out between 253 and 463 K at a heating rate of 10 K/min.

DSC of the Cryoground Sample. About 5 mg of cryoground GCM was heated at 10 K/min from 253 to 463 K (a temperature above its melting point). It was observed that the amorphous sample exhibits a glass transition (T_g = 338 K; determined as the midpoint of the glass transition step in the thermogram) in its DSC that was followed by a recrystallization exotherm in the temperature range of 383−413 K and a melting endotherm in the temperature range of 421−443 K.

The melted sample was cooled down to 253 at 30 K/min in order to re-form the amorphous GCM *in situ* in DSC. This re-formed GCM was reheated at 10 K/min. The DSC thermogram of this quench-cooled melt of the cryoground

GCM exhibited a T_g) at the same temperature (338 K) as before and exhibited no recrystallization events on heating up to the melting temperature.

DSC of the Quenched Sample (Obtained by Quench-Cooling of the Melt of Crystalline GCM on the Capacitor Plate). About 5 mg of quenched GCM was heated at 10 K/min from 293 to 463 K.

Infrared Spectroscopy (FT-IR) Measurements. FT-IR spectra were obtained using a Bio-Rad FTS-6000 spectrometer equipped with an UMA-500 infrared microscope. The microscope had a 250 × 250 mm mercury cadmium telluride detector (MTC) that was cooled to 77 K using liquid nitrogen. The spectra were obtained in the wavenumber range of 4000−700 cm^{-1} with a resolution of 4 cm^{-1}. The interferograms were recorded by accumulating 128 scans. FT-IR spectra were obtained on single grains of crystalline (about 100 × 100 μm) and milled (about 100 × 100 μm) GCM. In addition, a routine FT-IR spectrum of a GCM solution in n-butanol was collected using a diamond ATR accessory.

Broadband Dielectric Spectroscopy (BDS) Measurements. Dielectric measurements of quenched GCM were performed over a wide frequency range from 10^{-2} to 10^9 Hz. Isobaric dielectric measurements at ambient pressure from 10^{-2} to 10^7 Hz were carried out using a Novo-Control GMBH Alpha dielectric spectrometer. Using Agilent 4291B impedance analyzer connected with Novo-Control GMBH system, we were able to measure dielectric spectra in the high frequency range from 10^6 to 10^9 Hz. For the isobaric measurements, the sample was placed between two stainless steel electrodes of the capacitor with a gap of 0.176 mm. However, in the case of high frequency measurements the sample was placed between two gold-plated electrodes (diameter, 5 mm; gap, 0.05 mm). Using these two methods, the dielectric spectra of quenched GCM were collected in a wide temperature range from 201.15 to 453.15 K. The temperature was controlled by the Novo-Control Quattro system, with the use of a nitrogen gas cryostat. Temperature stability of the samples was better than 0.1 K. In the case of the cryoground GCM, dielectric measurements were carried out only over the frequency range of 10^{-2} −10^7 Hz. The milled sample was placed between two stainless steel electrodes (diameter 20 mm) of the capacitor with a gap of 0.1 mm. BDS spectra of cryomilled sample were collected in a temperature range of 201.15−387.15 K.

Nuclear Magnetic Resonance (NMR) Spectroscopy Measurements. High-resolution ^{1}H, ^{13}C, and 2D-COSY NMR experiments were carried out on a Varian 600 NMR spectrometer equipped with a 5-mm probe, in DMSO-d_6 solution at 299 K. The ^{1}H NMR spectra were acquired with 16−64 scans, 10.8 kHz spectral width and 128 K data points, giving a digital resolution of 0.08 Hz. The ^{13}C spectra were accumulated with 1000−2000 scans using a spectral width of 37.8 kHz and 64 K data points, and using WALTZ-16 decoupling. The FIDs were zero-filled to 128 K, giving a digital resolution of 0.58 Hz. The chemical shifts are expressed on the δ scale relative to internal TMS. NMR characterizations of both the crystalline GCM (amide) sample and the GCM sample heated for 1 h at its melting point are presented below.

The Crystalline Sample of GCM Drug. ^{1}H assignment (DMSO-d_6, TMS) δ (ppm): 10.296 (bs, 1H, −SO_2−N*H*CO−); 8.257 (t, 1H, −CO−N*H*−CH_2CH_2−, J = 5.6 Hz); 7.839 (AA′, 2H, H-2′$_{arom}$, H-6′$_{arom}$, J_{AX} = 8.4 Hz); 7.637 (d, 1H, H-6$_{arom}$, $J_{4,6}$ = 2.8 Hz); 7.497 (dd, 1H, H-4$_{arom}$, $J_{3,4}$ = 8.9 Hz, $J_{4,6}$ = 2.8 Hz); 7.488 (XX′, 2H, H-3′$_{arom}$, H-5′$_{arom}$, J_{AX} = 8.4 Hz); 7.149 (d, 1H, H-3$_{arom}$, $J_{3,4}$ = 8.9 Hz); 6.324 (d, 1H, −CO−N*H*−C_6H_{11}, $J_{1'',NH}$ = 7.8 Hz); 3.796 (s, 3H, O*C*H_3); 3.550 (td, 2H, −CO−NH−*C*H_2−CH_2−, J = 7.0 Hz, J = 5.6 Hz); 3.276 (m, 1H, H-1″); 2.935 (t, 2H, −CO−NH−CH_2−*C*H_2−, J = 7.0 Hz); 1.681−1.445 (m, 5H, 5 × H$_{cyclohexyl}$); 1.262−1.047 (m, 5H, 5 × H$_{cyclohexyl}$).

^{13}C assignment (DMSO-d_6, TMS) δ (ppm): 163.528 (1C, −*C*O−NH−CH_2CH_2−); 155.588 (1C, C-2$_{arom}$); 150.323 (1C, −NH−*C*O−NH−); 145.104 (1C, C-1′$_{arom}$); 138.091 (1C, C-4′$_{arom}$); 131.385, 129.393, 129.170, 127.185, 124.756, 124.235 (8 × C, C-1$_{arom}$, C-4$_{arom}$, C-5$_{arom}$, C-6$_{arom}$, C-2′$_{arom}$, C-3′$_{arom}$, C-5′$_{arom}$, C-6′$_{arom}$); 114.057 (1C, C-3$_{arom}$); 56.116 (1C, −O*C*H_3); 47.962 (1C, C-1″); 40.045 (1C, −CO−NH−*C*H_2−CH_2−); 34.557 (1C, −CO−NH−CH_2−*C*H_2-); 32.158 (2C, C-2″, C-6″); 24.870 (1C, C-4″); 24.058 (2C, C-3″, C-5″).

The GCM Sample Heated at Its Melting Point for 1 h. ^{1}H assignment (DMSO-d_6, TMS) δ (ppm): 8.263 (t, 1H, −CO−N*H*−CH_2CH_2−, J = 5.6 Hz); 7.774 (AA′, 2H, H-2′$_{arom}$, H-6′$_{arom}$, J_{AX} = 8.3 Hz); 7.652 (d, 1H, H-6$_{arom}$, $J_{4,6}$ = 2.8 Hz); 7.500 (dd, 1H, H-4$_{arom}$, $J_{3,4}$ = 8.9 Hz, $J_{4,6}$ = 2.8 Hz); 7.453 (XX′, 2H, H-3′$_{arom}$, H-5′$_{arom}$, J_{AX} = 8.3 Hz); 7.302 (s, 2H, −SO_2N*H*$_2$); 7.156 (d, 1H, H-3$_{arom}$, $J_{3,4}$ = 8.9 Hz); 3.814 (s, 3H, O*C*H_3); 3.540 (td, 2H, −CO−NH−*C*H_2−CH_2−, J = 7.1 Hz, J = 5.6 Hz); 3.276 (m, 1H, H-1″); 2.918 (t, 2H, −CO−NH−CH_2−*C*H_2−, J = 7.1 Hz).

^{13}C assignment (DMSO-d_6, TMS) δ (ppm): 163.500 (1C, −*C*O−NH−CH_2CH_2−); 155.588 (1C, C-2$_{arom}$); 143.527 (1C, C-1′$_{arom}$); 142.028 (1C, C-4′$_{arom}$); 131.395, 129.405 (2C, C-4, C-6); 129.073, 125.598 (2 × 2C, C-2′$_{arom}$, C-3′$_{arom}$, C-5′$_{arom}$, C-6′$_{arom}$), 124.756, 124.235 (2 × C, C-1$_{arom}$, C-5$_{arom}$); 114.060 (1C, C-3$_{arom}$); 56.171 (1C, −O*C*H_3); 40.247 (1C, −CO−NH−*C*H_2−CH_2−); 34.503 (1C, −CO−NH−CH_2−*C*H_2−).

Results and Discussion

Part A: Study of the GCM Sample Obtained by Quench-Cooling. In order to confirm the amorphous nature of the quenched material, the XRD technique was applied. It is well-known that XRD is one of the most definitive methods for detecting and quantifying molecular order in a system. As there is no long-range three-dimensional molecular order associated with a material in the amorphous state, the diffraction of the electromagnetic radiation is irregular when compared to that in the crystalline state. Thus, the very broad peaks observed as a blue line in Figure 2, compared to the sharp peaks typical for the crystalline state (black line

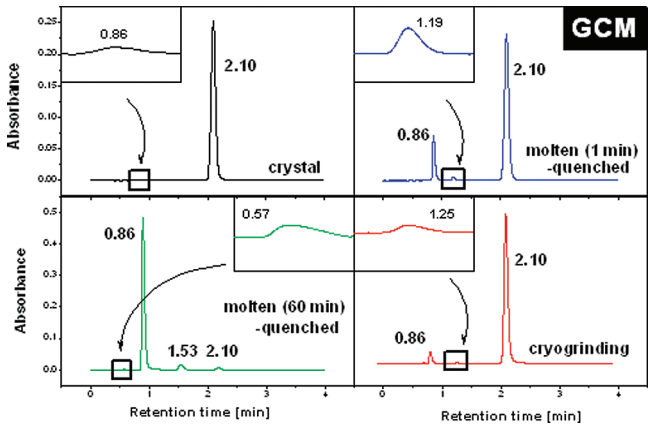

Figure 3. UPLC chromatogram of glibenclamide: crystalline (black line); heated at the melting point for 60 min and then quenched (green line); molten for 1 min and next quick quenched (blue line); obtained by cryogenic grinding (red line). All peaks, except for that with t_R = 0.57 min, are characteristic for UV spectra of GCM drug.

in Figure 2), indicate that the sample under test has indeed an amorphous form. As it was found by Hassan et al., the conversion from the crystalline to the glassy state in GCM drug is connected with the transition between two constitutional isomers, namely, between the keto and enol forms. However, taking into account the types of bonds existing in the crystalline and glassy states of the examined drug, one can say that this terminology is not adequate. In our opinion, the transition observed in GCM should be rather called an *amide−imidic acid tautomerism* instead of a *keto−enol* one.

Test of Chemical Decomposition. As mentioned in the Introduction, there are contradictory literature reports about the possible decomposition of GCM during melting. In order to clarify these discrepancies, UPLC and FT-IR methods were employed.

Using the UPLC technique, we analyzed crystalline GCM and two amorphous samples that have different melting rates. The chromatogram of crystalline GCM was used for further analysis as a reference. As displayed in Figure 3, it consists of two peaks: one that is pronounced and the other that is small with retention times of 2.10 and 0.86 min, respectively. It has been reported that the most stable form of GCM is the amide form (see Figure 1a) and therefore one can suppose that the greater peak comes from this form of the GCM molecule. As stated previously, conversion to the glassy state by dissolution of GCM leads to an equilibrium between the two easily interconvertible constitutional isomers. Thus, the second peak detected in the chromatogram of the crystalline sample suggests that a less stable imidic acid form of the drug exists in the tested solution. It is important to note here that both of the recorded peaks have similar associated UV spectra as characteristic of the GCM drug. Hence, one can be sure that the sample under test is indeed a pure GCM crystal.

In the next step, two amorphous GCM samples were prepared. The first portion of the crystals was melted and held at the melting temperature for one minute whereas the second one was held at the same temperature for an hour. Subsequently, both of them were rapidly quenched and were further analyzed by the UPLC method. The chromatogram of the first amorphous material is depicted as a blue line in Figure 3. As can be noted, there are three peaks with retention times of 2.10, 0.86, and 1.19 min, respectively. It is clearly obvious that the retention times of the first and the second peaks are exactly the same as those observed in the chromatogram of the crystalline GCM; however, the areas under these peaks are different. The third peak with the retention time equal to 1.19 min was not observed in the chromatogram of the crystalline GCM. It should be stressed that the first sample has a UV spectrum that is characteristic of GCM. Therefore, this new peak should have arisen from one of the possible imidic acid forms. Because three peaks (t_R = 2.10, 0.86, and 1.19 min) were observed in the amorphous form of the drug, one can suppose that there are three isomers of GCM coexisting in the glassy state (see Figure 1). Independent of the number of possible imidic acid forms, the UPLC method demonstrated that the quenched material was chemically pure. Thus, we can state that the thermal decomposition of GCM drug does not occur during the short melting time. Our result is at odds with the finding presented by Patterson et al. The authors had claimed that, during melting, GCM underwent an unacceptable degree of chemical degradation (16.4%). It is interesting that, from the analysis of the integral intensities of the UPLC peaks, we deduce that in fact 84.25% of the total peak area is connected to the amide form and the rest (15.75%) is associated with the imidic acid form of GCM (see Table 1). Therefore, it is possible that Patterson et al.'s interpretation of the chromatograms of the molten GCM is erroneous and that the authors perhaps treated the tautomers as the products of the thermal decomposition of the examined GCM drug.

Table 1. UPLC Analysis of All Examined Samples

analyzed sample	retention time [min]	ratio of products [%]
crystal	0.86	0.14
	2.10	99.86
molten (1 min)-quenched	0.86	14.42
	1.19	1.33
	2.10	84.25
cryogrinding	0.86	5.02
	1.25	0.26
	2.10	94.66
molten (60 min)-quenched	0.57	0.19
	0.86	89.63
	1.53	4.95
	2.10	5.23

Further tests have also shown that the thermal degradation of GCM does not occur even when the sample is annealed at its melting temperature for a longer time, i.e. 5 and 10 min. Some decomposition of GCM was detected only after 60 min at the melting temperature. At first sight, it is apparent that the sample, after 60 min of thermal exposure, starts to turn brown and lose its transparency. In addition, we start

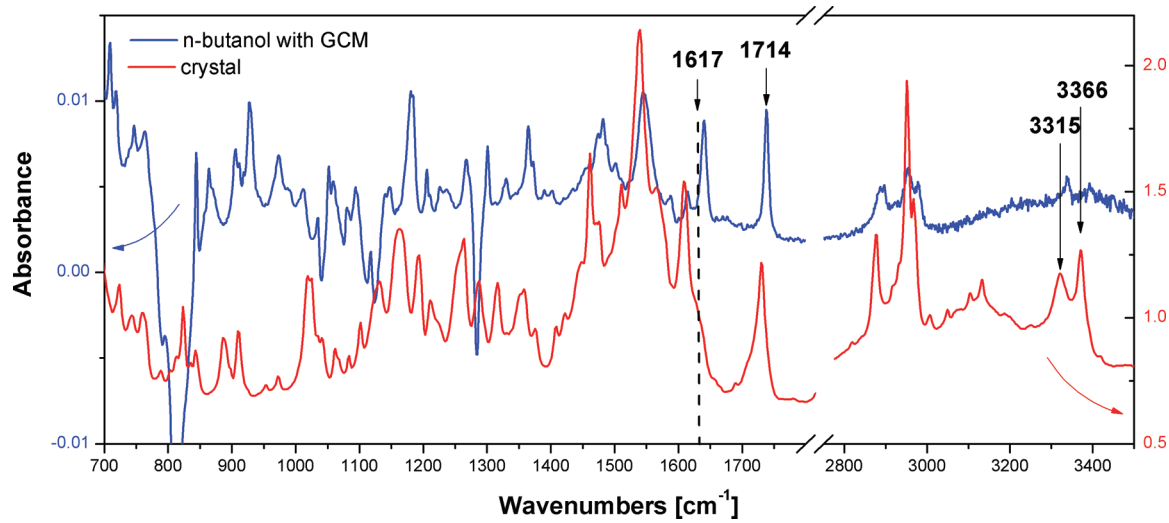

Figure 4. FT-IR of solution of GCM with *n*-butanol is depicted as a blue line, while the red line indicates the spectrum of crystal material. Solid arrows at 1717 and 3315 cm^{-1} indicate bands that decrease after amorphous conversion.

to observe new Bragg peaks in its XRD spectrum, which is indicative of the production of an additional unidentified substance in the sample (see the green line in Figure 2). It becomes also evident from the registered UPLC chromatogram that this sample is partially decomposed. In Figure 3, one can clearly identify a new peak in the UPLC chromatogram (with $t_R = 0.57$ min). Moreover, the UV spectrum of the sample is different from that of the pure GCM drug. In addition, one can also observe a significant shift of the peak detected previously at a $t_R = 1.19$ min toward a longer retention time ($t_R = 1.53$ min).

To characterize the amorphous GCM in more detail, FT-IR spectroscopy was applied to it in a wide temperature range. Since this technique is very sensitive to structural changes occurring in a sample, at first we analyzed the infrared characteristics of the GCM crystal as a reference. The FT-IR spectrum of crystalline GCM is presented in Figure 4. It is worth nothing that our FT-IR spectrum is similar to the spectrum published by Panagopoulou-Kapalani et al.[16] In accordance with the interpretation of the FT-IR spectra presented in works 16–18, two characteristic peaks were observed in our GCM FT-IR spectrum at 3315 and 3366 cm^{-1} that correspond to the amide stretching band associated with the amide moiety and urea group, respectively (Figure 4). The next sharp peak is visible at 1714 cm^{-1} and is associated with the carbonyl stretching vibration which occurs at the sulfonylurea end of the molecule. The second benzoyl carbonyl stretching band is weakly visible in the crystal's FT-IR spectrum. Thus, the FT-IR measurement for a solution of *n*-butanol and GCM was performed (see the bold blue line in Figure 4). Consequently, it has been clearly visible that there is a band at 1615 cm^{-1}, which is assigned to the C═O bond.

As stated previously, it has been reported that when GCM is transformed to its amorphous form, it undergoes a transition from the amide form to mostly the imidic acid form. The spectrum of quenched GCM is shown as a dotted blue line in Figure 5. It is obvious from the spectrum that a general reduction in the intensity of the bands and the loss of spectral resolution occurs upon quenching. Both of these effects are attributed to the drug amorphization process. Moreover, there are a few distinct differences between the crystalline and amorphous FT-IR spectra of GCM. First of all, the N−H band detected at 3315 cm^{-1} in the crystalline sample is found to mostly disappear in the amorphous form, while the N−H stretch of the urea group at 3376 cm^{-1} remains mostly unchanged: it is seen to only become slightly broader and shift slightly to higher wavenumbers. The next difference is that of a significant loss in the intensity in the carbonyl stretching region of the spectrum of the quenched sample. Apart from a decrease in the carbonyl band intensity, a new band at 1637 cm^{-1} is also found to appear. According to the literature data, this new band is attributed to a C═N stretch. Thus, it is a result of the amide−imidic acid conversion between the crystalline and glassy GCM. The alluded complete disappearance of the N−H band serves as further evidence that the tautomerism occurs during the quenching of the molten sample. Moreover, it is important to mention that the amorphous GCM undergoes some changes in the fingerprint region around 1020 and 1295 cm^{-1}, respectively. However, there were no changes in the symmetric and asymmetric sulfonyl stretching positions at 1307 and 1158 cm^{-1}, respectively. In this connection, Hassan et al.[8] have suggested that there are potentially two positions in the examined molecule where the tautomerism could occur: at the amide moiety (see Figure 1b) and at the sulfonylurea end of the molecule (see Figure 1c). According to the interpretation of IR data presented in works 8 and 17 our findings indicate also that there is no imide formation in the sulfonylurea part of the molecule. This suggests that only one imidic acid form exists in the glassy state, and has a structure as depicted in Figure 1b. However, when the UPLC results are taken into consideration, one can suppose that more than one type of imidic acid form is possible in the

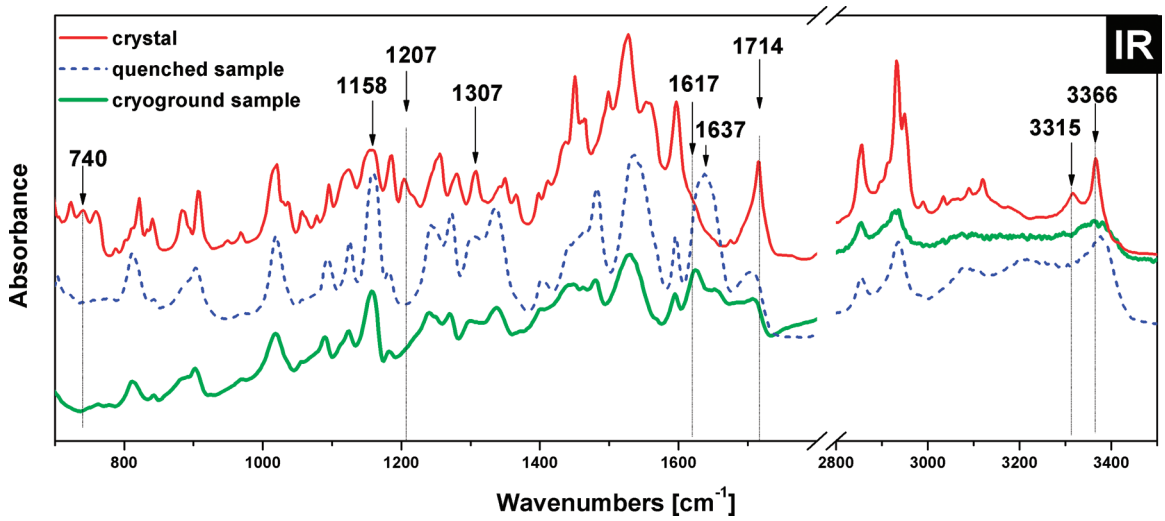

Figure 5. IR spectra of glibenclamide: crystalline (red thin line), obtained by quench-cooling (blue dotted line), obtained by cryogenic grinding (bold green line). All spectra were collected at room temperature. Solid arrows indicate the main changes between the crystal and glassy samples (see text).

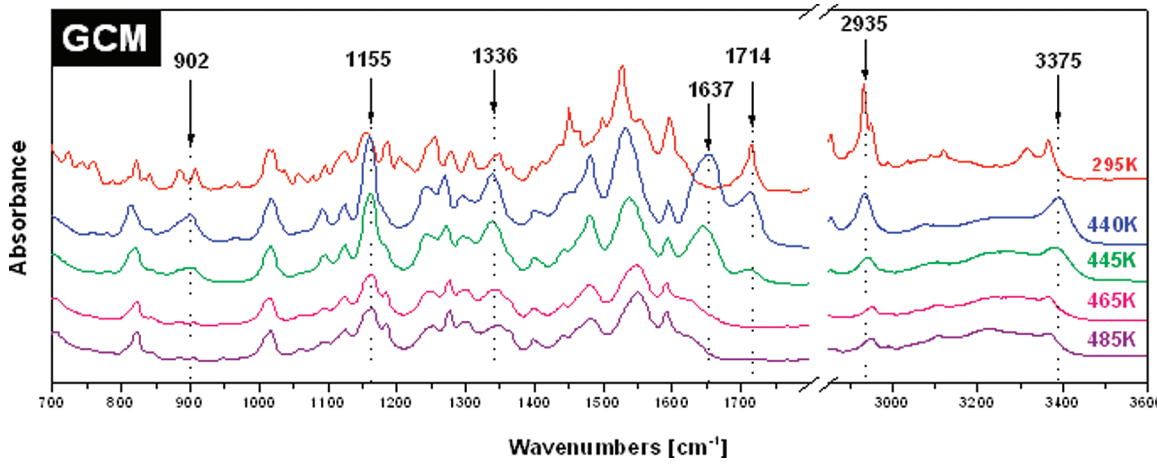

Figure 6. FT-IR spectra collected during annealing of the GCM at 295, 440, 445, 465, and 485 K. Dotted lines indicate bands undergoing changes during annealing.

quenched GCM. A more detailed analysis of the tautomeric equilibrium detected in this drug will be presented elsewhere. At the moment, we are mainly interested in applying FT-IR measurements to verify if and when the thermal decomposition of the examined GCM drug occurs.

FT-IR spectra were also measured for a GCM sample in the temperature range of 295−485 K. The sample was initially heated from room temperature (298 K) to its melting point (440 K), and the spectra were collected at successive temperatures in steps of 10 K. After this, the GCM sample was heated from 445 to 485 K, and the spectra were recorded every 20 K. Figure 6 shows the infrared spectra of GCM at room temperature (295K) and at the temperatures of 440, 445, 465, 485 K. Since there were no significant differences in the spectra registered in the temperature range 295−430 K, these data are not presented here. The main changes were observed in the spectral shape. For example, the broadening of the bands due to the softening and/or hardening of various vibrational modes are due to temperature effects. It is clearly obvious that at the melting point ($T = 440$ K), a conversion from the amide to the imidic acid form begins. Furthermore, a comparison of the liquid phase spectra collected at the temperatures 445 and 465 K exhibits dramatic intensity changes of the bands at 1155 (assigned to the two rocking CNH vibrations at the sulfonylurea end of the molecule), 1336 (connected with the twisting CH_2 vibrations existing in the middle of the GCM molecule), 2935 (assigned to the symmetric CH_2 vibration in cyclohexane) and 3375 cm^{-1} (as stated previously). On the other hand, some of the bands observed for the molten sample have disappeared at 465 K, namely, at 902 cm^{-1} and 1714 cm^{-1} assigned to the twisting CH_2 bonds in cyclohexane and connected with symmetric C═O vibrations at the sulfonylurea region, respectively. Based on the above results, we can state that GCM is stable up to 20 K above its melting point. The significant changes in the FT-IR spectrum registered above 460 K suggested that the examined sample could have been partly decomposed under these temperature conditions.

The preceding observation makes it relevant to pose the question: *How long is the GCM sample stable at the melting*

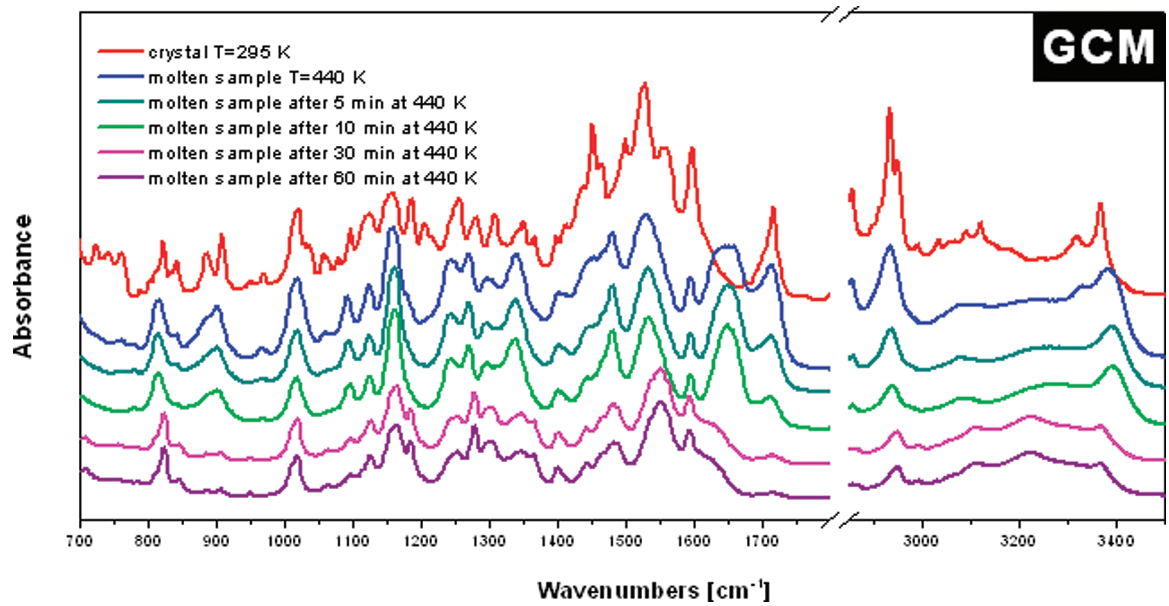

Figure 7. FT-IR spectra of GCM sample heated at the melting point for 1, 5, 10, 30, 60 min, respectively. As a reference the spectrum of crystal recorded at room temperature is presented as a red line.

point? To ascertain it, the examined material was heated to the 440 K and then annealed at this temperature for 1 h. The spectra were collected after 5, 10, 30, and 60 min, respectively. As can be seen in Figure 7 the spectra recorded after 30 and 60 min of heating exhibit some degradation (compared to the spectrum in Figure 6 collected at 485 K). This was also confirmed by NMR measurements. We have determined that the GCM sample annealed at the T_m for 1 h contains molecules in which N−S bonds were broken (a detailed NMR description of this sample is presented in the Experimental Section). Based on all of the preceding discussed measurements (such as XRD, UPLC, FTIR and NMR), we can state that the chemical degradation of GCM as suggested in ref 17 does not occur at its melting point provided that the melting time is short enough. Thus, our analysis confirms that GCM is stable during the time required for complete melting of its sample.

Analysis of Molecular Dynamics in Quenched GCM. There are many experimental methods available for monitoring molecular dynamics in amorphous materials; e.g. dielectric relaxation, dynamic mechanical analysis, proton correlation spectroscopy, NMR etc. In our work we employed BDS to study the vitrification process of GCM. In addition, we used DSC measurements as a complementary means for determining the glass transition as well as melting and crystallization temperatures of the material.

Dielectric loss spectra (i.e., an imaginary part of dielectric permittivity plotted as a function of frequency) measured at ambient pressure above (panel a) and below (panel c) T_g are presented in Figure 8. Herein, T_g is defined as the temperature at which the dielectric relaxation time τ_α reaches 100 s. The T_g of GCM is 338.98 K. In the dielectric loss spectra collected above T_g, one can distinguish two dielectric processes; the dc conductivity which is connected with the translational motion of ions and the structural relaxation process related to the cooperative rearrangements of the GCM molecules. The dc contribution is visible at lower frequencies as a strong increase in the imaginary part of dielectric permittivity and follows ω^{-1} dependence according to the electrodynamic relation

$$\varepsilon'' = \sigma/\varpi\varepsilon_0 \quad (1)$$

where ε_0 denotes the permittivity of vacuum. As shown in Figure 8a, in the frequency range from 10^{-1} to 10^{1} Hz, the structural relaxation peak becomes hardly apparent. Therefore, the identification of the maximum of peak position in this region is very difficult. The strong contribution of dc conductivity observed in the examined sample is characteristic of most pharmaceutical systems. For example, such contributions have been observed in the ε'' spectra of telmisartan[21] or indomethacin.[22] However the dc conductivity can be subtracted from the total dielectric loss spectrum using the above relation (eq 1). In the following analysis we discuss dielectric spectra in which the dc-conductivity contribution has been subtracted (see Figure 8b).

Figure 8b clearly shows that the α-relaxation peak shifts toward low frequencies with a lowering of the temperature and moves out the frequency measurement window below T_g. On the other hand, the secondary relaxation, called the γ-process, becomes apparent below T_g (see Figure 8c). Similar to the mentioned structural relaxation, the γ-process also slows down during cooling, but it is far less sensitive to temperature. For the γ-process to move over 6 decades in frequency, it is necessary to decrease the temperature by

(22) Wojnarowska, Z.; Adrjanowicz, K.; Wlodarczyk, P.; Kaminska, E.; Kaminski, K.; Grzybowska, K.; Wrzalik, R.; Paluch, M.; Ngai, K. L. Broadband Dielectric Relaxation Study at Ambient and Elevated Pressure of Molecular Dynamics of Pharmaceutical: Indomethacin. *J. Phys. Chem B* **2009**, *113* (37), 12536–12545.

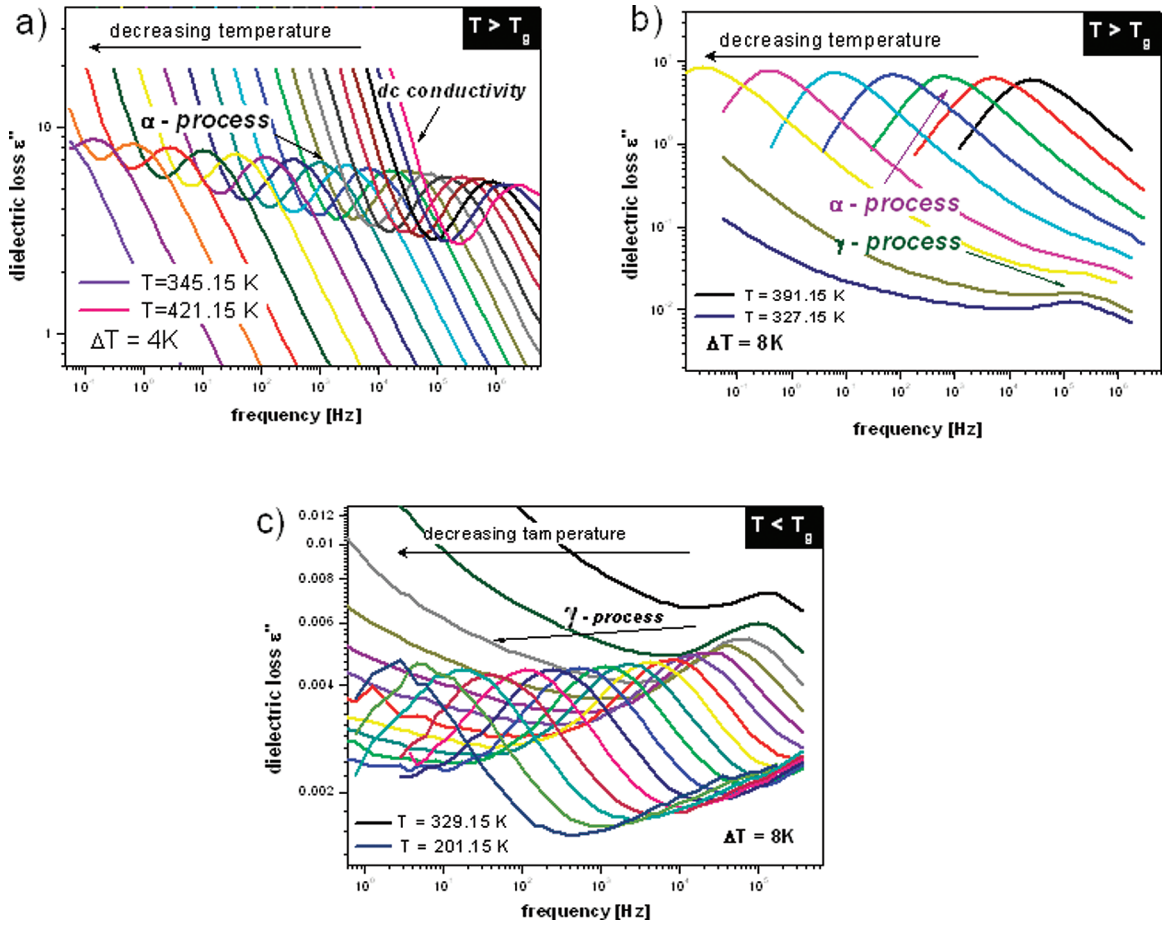

Figure 8. Dielectric loss spectra of glibenclamide obtained at ambient pressure. Panel (a) presents dielectric loss above the glass transition temperature. In panel (b) several spectra between temperatures 391.15 and 327.15 K, after subtracting the conductivity, are depicted, whereas in panel (c) dielectric loss spectra below T_g are presented.

more than 120 degrees, from 329 to 201 K. The nature of this secondary relaxation process will be discussed in the latter part of this paper.

In order to check whether or not the shape of the α-relaxation process is temperature invariant, we superimposed a number of dielectric loss peaks measured at different temperatures (both above and below T_g), using the spectrum obatined at $T = 351.15$ K as the reference one. The obtained masterplot (Figure 9) clearly shows that the shape of the α-process is practically invariant upon cooling. Thus, the time−temperature superposition principle is valid in the case of GCM.

The master curve presented in Figure 9 was next fitted by the one-sided Fourier transform of the Kohlrausch−Williams−Watts function[23,24]

$$\phi(t) = \exp[-(t/\tau_\alpha)^{\beta_{KWW}}] \qquad (2)$$

where t is time, τ_α is the characteristic relaxation time, and β_{KWW} ($0 < \beta_{KWW} \leq 1$) denotes the stretching parameter that describes the shape of the spectrum. From fitting the experimental data presented in Figure 9 to eq 2, the value of the exponent β_{KWW} was estimated to be 0.74. Thus, the

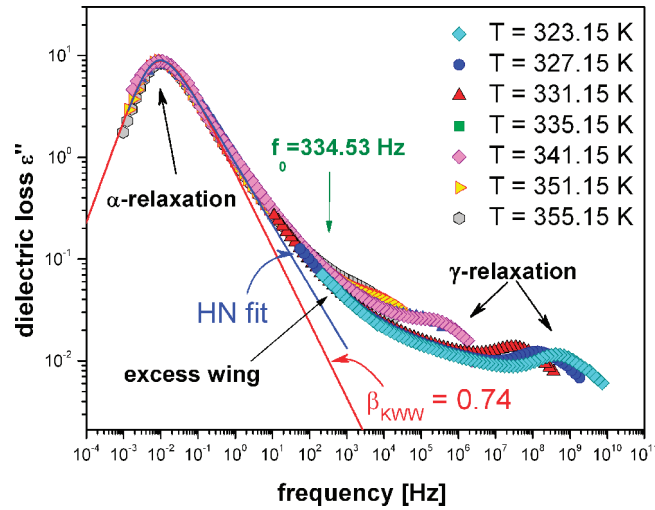

Figure 9. Superimposed dielectric spectra of GCM taken at ambient pressure (p = 0.1 MPa), at seven different temperatures above and below T_g. The solid red line is a KWW function with $\beta_{KWW} = 0.74$, while the blue line is a Havriliak−Negami fit. The green arrow denotes the position of the primitive relaxation predicted from eq 7 at 341.15 K.

(23) Kohlrausch, R. Nachtrag über die elastiche Nachwirkung beim Cocon und Glasladen. *Ann. Phys. (Leipzig)* **1847**, *72*, 393.

loss curve is broader than the classical Debye response by about 1.43 times. The practical meaning of the β_{KWW} parameter was invoked in literature implying that it is directly connected with the stability of amorphous systems. Shamblin et al.[25] has suggested that the stability of various amorphous drugs should improve with the narrowing of the α-peak. According to this criterion, the amorphous GCM can be considered as a stable system and it should not reveal any tendency to crystallization. This is a fundamental issue for the pharmaceutical industry because there is a general problem with producing stable forms of amorphous drugs.

The dielectric α-relaxation peak can be also analyzed by means of the Havriliak−Negami function[26] (eq 3), that enables a slightly better fit of the experimental data

$$\varepsilon^*(\varpi) = \varepsilon_\infty + \frac{\Delta\varepsilon}{[1 + (i\omega\tau_{HN})^{\alpha_{HN}}]^{\beta_{HN}}} \quad (3)$$

where ε_∞ is the limiting high-frequency permittivity and τ_{HN} denotes a characteristic relaxation time, whereas α and β parameters characterize the shape of the dielectric loss curve. The representative HN fit is depicted as a blue line in Figure 9. The shape parameters α_{HN} and β_{HN}, determined also from fitting analysis, are equal to 0.95 and 0.63, respectively. In order to describe the secondary relaxation, we have used the Cole−Cole function[27] ($\beta_{HN} = 1$) with the α_{HN} parameter being approximately equal to 0.63. The temperature dependencies of the characteristic relaxation time in both of the relaxation phenomenon processes are presented in Figure 10.

In the vicinity of T_g, the temperature dependence of α-relaxation time is usually fitted with the Vogel−Fulcher−Tamman (VFT) equation[28−30]

$$\tau_\alpha = \tau_\infty \exp\left(\frac{D_T T_0}{T - T_0}\right) \quad (4)$$

The dependence log $\tau_\alpha(T)$ for GCM can be satisfactorily described over the entire measured range of temperatures by a single VFT equation with the following fitting parameters: log $\tau_\infty = -15.63 \pm 0.13$, $D_T = 11.95 \pm 0.35$ and $T_0 = 261.92 \pm 1.43$ K. Based on the VFT fits, the T_g of GCM was estimated to be 338.98 K. As the T_g of GCM is almost 45 K higher than ambient temperature, it should guarantee the stability of the amorphous phase of GCM under normal handling conditions.

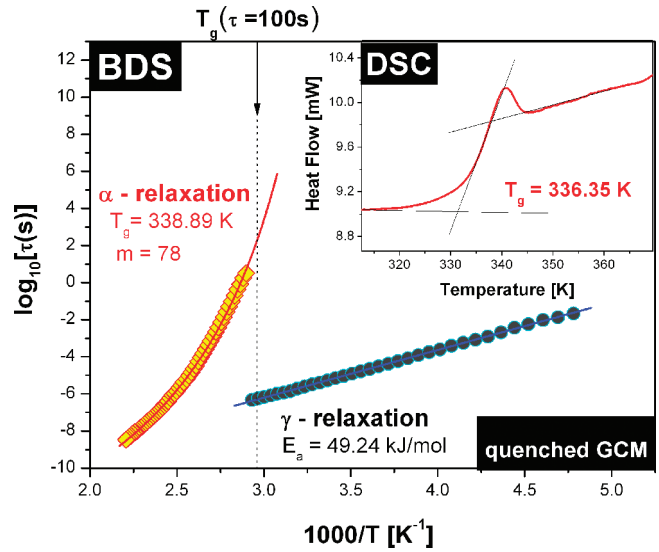

Figure 10. Relaxation map of the GCM. Blue circles and yellow squares denote structural and γ-relaxation times, respectively. Solid lines are VFT and Arrhenius fits to $\tau_\alpha(T^{-1})$ and $\tau_\gamma(T^{-1})$, respectively. In the inset panel standard DSC measurements of GCM with the heating rate 10 K/min are presented.

The T_g of GCM was also determined using DSC technique. The DSC curve obtained during the heating of amorphous GCM is depicted in the inset panel of Figure 10. There is a characteristic signature for the T_g in the heat flow with an onset at 336.15 K. We found that the value of T_g as determined from BDS and DSC measurements differed only by 3 K. This small discrepancy probably results from the different heating rates used in DSC and BDS experiments.

We also note here that the T_g of GCM determined from our BDS and DSC measurements is significantly different (almost 10 K) from the value reported by Patterson et al.[17] They obtained T_g for the ball milled and quench-cooled GCM to be 343 and 323 K, respectively, from DSC studies. The authors had attributed this considerable difference between the T_g of the ball milled and quench-cooled GCM samples to chemical degradation. However, as discussed in the previous section, thermal decomposition of GCM does not occur at its melting temperature. Based on this fact, the attribution of the difference in T_g to chemical degradation offered by the authors of ref 17 appears to be erroneous. On the other hand, our studies show that the amide and imidic acid forms of GCM have different physical properties, including T_g. Hence, we believe that the mentioned difference in T_g is possibly due to the different tautomers present in the supercooled liquid of GCM.

The most characteristic feature of molecular dynamics in vitrifying liquids is a systematic deviation of τ_α from the Arrhenius law. However, the degree of this deviation varies from one compound to another. The steepness index is a

(24) Williams, G.; Watts, D. C. Non-symmetrical dielectric relaxation behavior arising from a simple empirical decay function. *Trans. Faraday Soc.* **1970**, *66*, 80–85.
(25) Shamblin, S. L.; Hancock, B. C.; Dupuis, Y.; Pikal, M. J. Interpretation of relaxation time constants for amorphous pharmaceutical system. *J. Pharm. Sci.* **1999**, *89*, 417–427.
(26) Havriliak, S.; Negami, S. A complex plane representation of dielectric and mechanical relaxation processes in some polymers. *Polymer* **1967**, *8* (4), 161.
(27) Cole, K. S.; Cole, R. H. Dispersion and absorption in dielectrics I. Alternating current characteristics. *J. Chem. Phys.* **1941**, *9*, 341.
(28) Vogel, H. The law of the relation between the viscosity of liquids and the temperature. *Phys. Z.* **1921**, *22*, 645–646.
(29) Fulcher, G. Analysis of recent measurements of the viscosity of glasses. *J. Am. Ceram. Soc.* **1925**, *8* (6), 339–355.
(30) Tammann, G.; Hesse, W. Die Abhängigkeit der Viscosität von der Temperatur bie unterkühlten Flüssigkeiten. *Z. Anorg. Allg. Chem.* **1926**, *156* (1), 245–257.

commonly used parameter to quantify the deviation of structural relaxation times from the Arrhenius behavior. It can be also calculated on the basis of VFT fit:[31]

$$m_P = \left.\frac{\partial \log_{10}(\tau)}{\partial(T_g/T)}\right|_{P=\text{const},T=T_g} = D_T\frac{T_0}{T_g}\left(1 - \frac{T_0}{T_g}\right)^{-2}\log_{10} e \quad (5)$$

where T_g is the glass transition temperature, and D_T and T_0 are VFT equation parameters.

This deviation is believed to play a crucial role in the case of amorphous drugs, because it can be used for establishing the appropriate storage conditions for a particular drug. In general, the fragility parameter defined by eq 5 describes the rapidity with which a liquid structure, which was arrested at the glass transition during cooling, becomes disrupted on reheating.[32] The typical values of fragility are between 16 and 200. The substances with small values of the steepness index, called "strong", exhibit almost the Arrhenius behavior of log $\tau_\alpha(T)$, whereas the glass forming liquids with large values of m_P, called "fragile", reveal an entirely non-Arrhenius dependence. The value of fragility of GCM was found to be 78, and it can be compared with other recently measured amorphous pharmaceuticals: verapamil hydrochloride[20] ($m_P = 88$), telmisartan[21] ($m_P = 87$) and indomethacin[22] ($m_P = 83$). Thus, GCM can be classified as an intermediate glass-former drug.

Now we focus on the analysis of the secondary relaxation process detected in the dielectric loss spectra of GCM. In the glassy state, the temperature dependence of the γ-relaxation times exhibits a linear dependence when log τ is plotted vs $1/T$ (see Figure 5). Thus, it can be described by using the Arrhenius power law:

$$\tau_\gamma = \tau_\infty \exp\left(\frac{E_a}{k_B T}\right) \quad (6)$$

in which τ_∞ is the preexponential factor, E_a is the energy barrier and R is the gas constant. The best fit was obtained for $\log_{10}\tau_\infty = -13.92 \pm 0.98$ and $E_a = 49.24 \pm 0.98$ kJ/mol. It has been recently established that there are two possible molecular origins for secondary relaxation observed in dielectric spectra. The former is related to molecular internal motion and basically does not provide any information about liquid−glass transition. However, the latter one, called the Johari−Goldstein (JG) process, originates from some local motions of the entire molecule. It is believed that this type of secondary process is a precursor of the α-relaxation. However, the JG relaxation process in many glass-forming liquids is not always visible as a well-separated peak in the dielectric spectra. There are a lot of experimental data that suggest that some relaxation process might be hidden under the α-peak. In such cases, the JG process is manifested as an extra contribution to the high frequency part of the α-relaxation peak. This deviation is known as an "excess wing" and is usually observed at frequency about two decades higher than the maximum of the α-process. Our measurements have determined that amorphous GCM is a new example of a system with an excess wing. In order to check if the excess wing can be identified with the JG relaxation process, we applied the coupling model (CM) prediction proposed by Ngai[34−37]

$$\tau_{JG} \approx \tau_0 = t_c^{\,n}\tau_\alpha^{\,1-n} \quad (7)$$

where τ_0 is so-called "primitive" relaxation time, t_c is the crossover time from independent relaxation to cooperative relaxation and is close to 2 ps, and n is a coupling parameter ($n = 1 - \beta_{KWW}$). Using the earlier found value of β_{KWW} and the value of the relaxation time determined from maximum of the α-peak at 341.15 K, we estimated the primitive relaxation time as $\tau_0 = 4.76 \times 10^{-4}$ s, which corresponds to the frequency $f_0 = 334.53$ Hz (see the green arrow in Figure 9). It is clearly seen that the determined value of f_0 is far from the maximum of the secondary γ-relaxation process and lies within the frequency range where the excess wing is observed. Thus, the excess wing is a hidden JG relaxation and is the precursor of the α-relaxation process. The other conclusion arising from this consideration is that the other secondary relaxation (γ) may originate from some intramolecular motion of a small part of the GCM molecule.

Part B: Study of GCM Sample Obtained by Cryogenic Grinding. UPLC and FT-IR Analysis of Milled Material. In order to confirm the amorphous nature of cryoground sample it was analyzed using the XRD method. The ground GCM as well as the previously analyzed molten-quenched material have a broad halo indicating that both samples are in the amorphous state. It is also clearly seen that the obtained diffraction intensities are exactly the same in both of the cases (see red line in Figure 2).

(31) Angell, C. A. Formation of glasses from liquids and biopolymers. *Science* **1995**, *267*, 1924.

(32) Angell, C. A. Shao, J. Grabow, M. In *Non-equilibrium phenomena in supercooled fluids, glasses and amorphous materials*, Proceedings of the International Workshop, Pisa, Italy, Sept 25–29, 1995; Giordano, M., Leporini, D., Tosi, M. P., Eds.; World Scientific: Singapore, 1996.

(33) Adrjanowicz, K.; Kaminski, K.; Paluch, M.; Wlodarczyk, P.; Grzybowska, K.; Wojnarowska, Z.; Hawelek, L.; Sawicki, W.; Lepek, P.; Lunio, R. Dielectric Relaxation Studies and Dissolution Behavior of Amorphous Verapamil Hydrochloride. *J. Pharm. Sci.* **2010**, *99* (2), 828–839.

(34) Ngai, K. L.; Paluch, M. Classification of secondary relaxation in glass-formers based on dynamic properties. *J. Chem. Phys.* **2004**, *120*, 857.

(35) Ngai, K. L., Rendell, R. W. Supercooled liquids, advances and novel applications. In *Supercooled liquids: Advances and novel applications*; Fourkas, J. T., Kivelson, D., Mohanty, U., Nelson, K., Eds.; ACS Symposium Series 676; American Chemical Society: Washington, DC, 1997; Chapter 4, p45.

(36) Ngai, K. L.; Tsang, K. Y. Similarity of relaxation in supercooled liquids and interacting arrays of oscillators. *Phys. Rev.* **1999**, *E60*, 4511–4517.

(37) Ngai, K. L. An extended coupling model description of the evolution of dynamics with time in supercooled liquids and ionic conductors. *J. Phys.: Condens. Matter* **2003**, *15*, S1107.

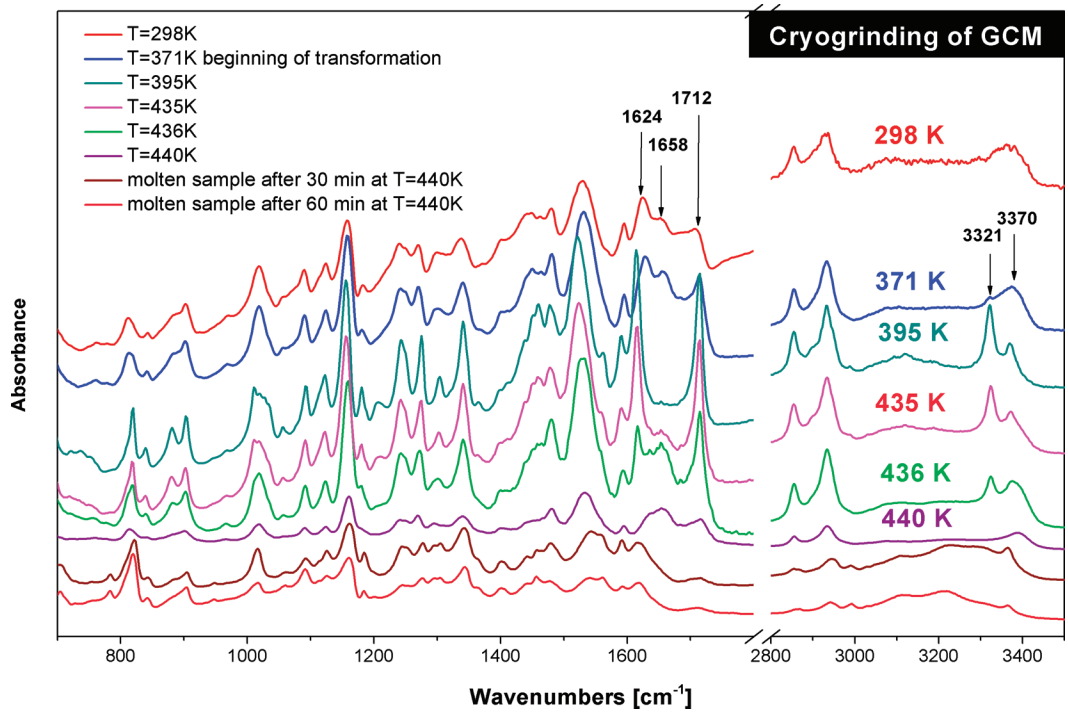

Figure 11. The red line indicates the FT-IR spectrum of GCM obtained by cryogenic grinding. The examined sample was next heated to 440 K and kept at this temperature for one hour. At the temperature equal to 371 K cryomilled GCM begins crystallize, while at 435 K it is molten.

Since CMM is a process carried out at very low temperatures, several literature reports indicate that the milled sample does not undergo any chemical degradation. To ascertain that the purity of milled GCM is unchanged, it was examined with the UPLC method. The analysis of the chromatogram showed that the sample did not contain any impurities. Similar to the crystalline GCM sample, the chromatogram of cryoground sample revealed one very pronounced peak with a retention time of 2.10 min and two additional minor peaks with retention times of 0.86 and 1.25 min (see Figure 3). However, similar to the quenched sample, all these peaks have UV spectra identical to those produced by crystalline GCM. The number of peaks visible in the UPLC chromatogram indicated that more than one imide isomer of GCM is present in the glassy state.

A further important question to pose is: *Does the amide−imidic acid tautomerism occur in the case of cryoground GCM?* It is well-known that cryogenic milling of the crystalline compounds well below their T_g is fundamentally different from the usual thermal quenching of the melt. As proven by Descamps,[38] caramelization and mutarotation processes do not occur in amorphous lactose obtained by milling. Based on this, one could suppose that the amide−imidic acid conversion would not be detected in the cryomilled GCM. However, the obtained UPLC chromatogram of cryoground GCM does not confirm this supposition. Since the two observed minor peaks in the UV spectrum are characteristic of the analyzed drug, we can associate them with the imide isomers of GCM. It is important to note here that the imidic acid form of analyzed sample has been observed after amorphization by using ball milling[17] as well as by quenching of the molten sample.[7]

FT-IR spectroscopy was exploited to characterize the structure of cryoground material in detail. The FT-IR spectrum of milled GCM is presented in Figure 5 together with the spectra obtained for the crystalline and quenched samples. It is clearly obvious that in the case of both of the amorphous materials a general reduction in the intensity of the bands can be observed in comparison to the crystalline GCM sample. However, one can see that the reduction of the bands is much greater for the ground GCM. As with the quenched GCM sample, the N−H stretching vibration at 3315 cm^{-1} is found to be absent in the sample upon cryomilling. There has also been a significant loss in intensity in the carbonyl stretching region of the spectrum. However, as contrasted with the quenched GCM, both of the C═O bands are clearly apparent. Furthermore, a new band attributed to a C═N stretch also appears in the spectrum. In addition, the milled sample is also found to have undergone changes in the fingerprint regions around 1020 and 1295 cm^{-1}. These changes in the FT-IR spectra indicate that the cryomilling of GCM leads to the conversion of the amide form to the imidic acid form, originating from the amide moiety of the GCM molecule.

To make our analysis more complete, we have measured the FT-IR spectra of the cryomilled GCM material in the temperature range of 295−437 K (see Figure 11). Initially,

(38) Descamps, M.; Willart, J. F.; Dudognon, E.; Caron, V. Transformation of pharmaceutical compounds upon milling and comilling: the role of T_g. *J. Pharm. Sci.* **2007**, *96* (5), 1398.

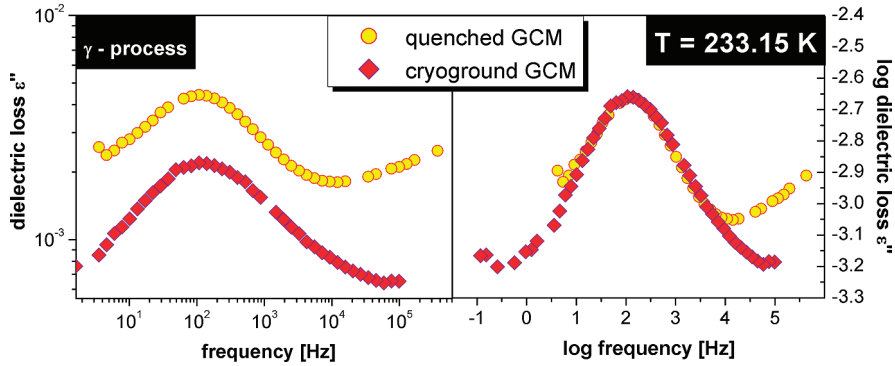

Figure 12. In the left panel representative dielectric measurement of γ-relaxation collected at 233.15 K is depicted as a red squares. Yellow circles indicate the spectrum recorded for quenched GCM at the same temperature conditions. The right panel shows the master curve constructed from the above-mentioned loss spectra in double logarithmic scale.

the cryomilled sample was heated to its melting point. A change in the initial FT-IR spectrum was first detected at 371 K. At this temperature, we can see an increase in the intensity of the two bands that are observed in the crystalline GCM, namely, the N−H stretching vibration at 3321 cm^{-1} and the amide carbonyl band at 1712 cm^{-1}. On the other hand, the band at 1658 cm^{-1} is seen to have disappeared. All together these changes indicate that, during heating, the tautomer formed upon milling reverts to the more stable amide form. The FT-IR spectrum of the recrystallized GCM is depicted as the green line in Figure 11. To ascertain that the examined sample is in the crystalline form, it was again characterized by XRD analysis. The obtained diffractogram confirmed that the material was indeed crystalline in nature. Moreover, it showed that the analyzed GCM sample had recrystallized to the same crystalline form as of the starting GCM material. Thus, the reappearance of the band at 3321 cm^{-1} could be used as an indicator of GCM recrystallization. This method has been used by Patterson et al.[17] to analyze the physical stability of GCM at different temperatures and humidity conditions.

Based on the liquid-phase FT-IR spectrum of GCM, as described previously, one could see that the current sample becomes molten at the 435 K (see the pink curve in Figure 11). Comparing this value with the T_m determined for the quenched GCM sample, we could determine that the T_m obtained for the milled material was lower by 5 K. To check as to how long the examined sample could be kept at the T_m without its decomposition, the following test was performed on the sample. The cryomilled GCM was heated to the 440 K and then kept at this temperature for 1 h. The FT-IR spectra were collected every 10 min. Since any significant changes in the FT-IR spectra were not observed after 10 and 20 min of heating, such data are not presented here. As can be seen in Figure 11, the spectra obtained after 30 and 60 min heating are quite similar to those obtained earlier for the quenched GCM sample (compare Figure 7). Therefore, in this case also, we have found that a partial decomposition of the GCM is possible if the sample is kept at T_m for a long enough time.

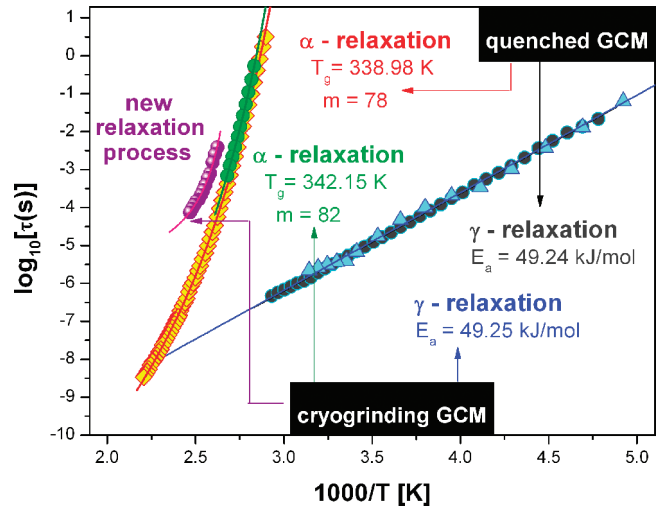

Figure 13. The relaxation map of GCM. $\tau_\alpha(T^{-1})$ of quench-cooling and cryogrinding are depicted as yellow squares and green circles, respectively, while the γ-relaxation times are visible as blue circles and blue triangles. Moreover the relaxation times of a new relaxation process detected above 381 K in the dielectric spectrum of milled sample are depicted as violet balls.

Molecular Mobility in Cryoground GCM. The dielectric loss spectra of cryomilled GCM were measured in the temperature range of 201.15−387.15 K, starting from the lowest temperature. A representative dielectric loss spectrum of the γ-relaxation process is displayed in Figure 12. As can be seen, its position as well as shape is identical with the spectrum collected at the same temperature for the quenched GCM sample. Moreover, the γ-peak also moves toward high frequency with increasing temperature. As in the case of the material obtained by quench-cooling, the $\tau_\gamma(T^{-1})$ dependence of cryomilled GCM satisfies the Arrhenius law. From the numerical fitting analysis, the preexponential factor $\log_{10}\tau_\infty = -13.90 \pm 0.18$ and activation energy $E_a = 49.25 \pm 0.84$ kJ/mol were determined (see Figure 13). It is apparent that there is no difference in the activation energy between the two samples. Thus, independent of the amorphization method, the γ-process detected in the dielectric loss spectra

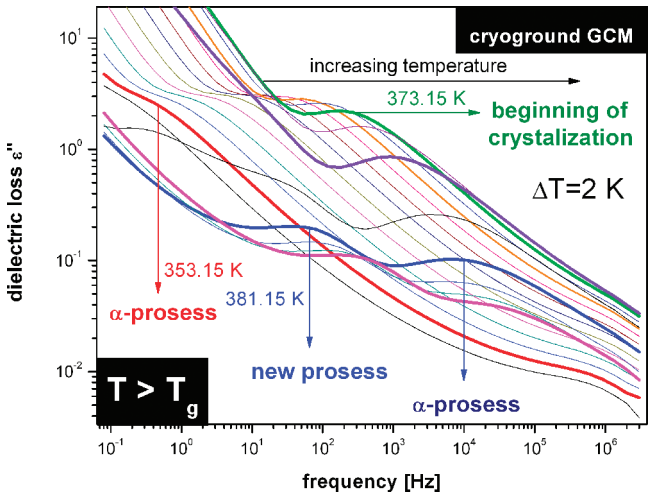

Figure 14. Dielectric loss curves for cryoground GCM collected above T_g. As can be seen at 381.15 K a new relaxation process has been detected.

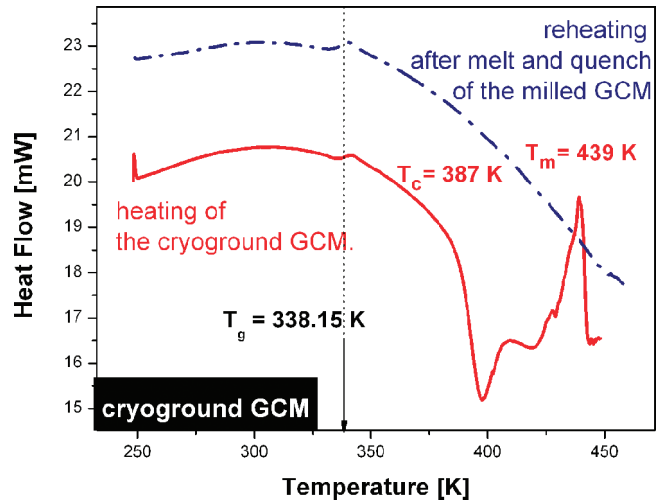

Figure 15. Solid red curve presents the temperature dependences of heat flow on heating of cryomilled GCM from room temperature to the melting points. The exothermic peak visible at 387 K is assigned to the cold crystallization of the examined sample. After melting, the sample was cooled down to room temperature (30 K/min) and next reheated (dashed blue line).

exhibited the same pattern of behavior, originating from the motion of a small part of the GCM molecule.

With increasing temperature, the γ-peak slowly disappears and the structural relaxation begins to appear in the experimental frequency window. In Figure 14, the imaginary part of dielectric permittivity plotted as a function of the frequency measured above T_g is presented. As can be seen, the maximum of the α-process appears in our frequency window at 353.15 K, i.e. at a temperature four kelvins higher than that for the quenched GCM sample. Moreover, we observed that the contribution of the dc conductivity is more pronounced in the dielectric spectra of cryoground GCM than in the case of the melt-quenched GCM. Additionally, we have compared the position and shape of the α-process measured for both samples. We have found that the structural relaxation detected in the milled material is slightly shifted toward the lower frequencies. This suggests that there is only a small discrepancy in the values of T_g of the two samples. However, the shapes of α-peaks obtained after subtracting the dc conductivity are essentially the same.

The temperature dependence of α-relaxation time determined as the inverse of the frequency of the maximum peak position, i.e., $\tau = (2\pi f_{max})^{-1}$, is presented in Figure 13. Similar to the case of quenched GCM, the $\tau_\alpha(T^{-1})$ dependence of cryomilled GCM exhibits a non-Arrhenius behavior which can be satisfactorily parametrized by means of eq 3. The best fit of the experimental data to VFT equation was achieved for the following set of parameters: $\log_{10}\tau_\infty = -14.71 \pm 0.68$, $D_T = 9.86 \pm 1.20$ and $T_0 = 272.37 \pm 4.58$ K. Using these parameters, one can easily determine the value of T_g as well as the fragility of cryomilled GCM. T_g was found to be 342.15 K, while $m_P = 82$. It is worth noting that this determined T_g value is in satisfactory agreement with that reported in ref 17 ($T_g = 343.15$ K). The fact that there is no significant difference between the T_g values estimated for both cryoground GCM and quenched GCM samples is another piece of evidence that the chemical decomposition of GCM does not occur during the melting process. Moreover, the T_g value for milled GCM evaluated on the basis of dielectric data analysis is very close to the T_g obtained from DSC measurement, $T_{gDSC} = 338.15$ K. Some of the DSC scans are shown in Figure 15. The examined sample also exhibits an exothermic peak in the temperature range of 383−413 K. This indicated that the molecules have sufficient kinetic energy at this temperature range to start the crystal growth process. This kind of phenomenon, usually called "cold crystallization", is frequently observed during the slow heating of glassy materials. A subsequent recrystallization event, occurring with an onset temperature around 373 K, was also observed during the BDS measurement of the cryomilled GCM. As can be seen in Figure 14, the crystallization process is manifested by a dramatic change in the dielectric response function, i.e., the intensity of the structural relaxation decreases due to a reduction in the density of mobile dipoles. It is worth reminding that the crystalline regions of the sample do not contribute to the dielectric response. Thus, one can observe a drop in the dielectric strength, $\Delta\varepsilon$, and consequently a reduction in ε''_{max}. In the final stages of the crystallization process at 381 K, a second peak was detected that was probably connected with the relaxation of the amorphous fraction constrained within the growing lamellae. The $\log_{10}\tau(1000/T)$ dependence estimated for this new relaxation process is displayed in Figure 13.

To gain more information about the crystallization of cryomilled GCM, we carried out the isothermal measurements at 373 K using the BDS method. We determined that the crystallization is complete only after 3 h under these temperature conditions. As in the case of nonisothermal crystallization, a reduction in the intensities of both the α-peak and the real part of the complex dielectric permittivity were observed.

It is also apparent that both the quench-cooled and the cryomilled GCM samples exhibit opposite tendencies to crystallization with an increase in temperature. The former is stable in a wide range of temperatures. We did not observe even a trace of crystallization during all of the measurements on this compound. The opposite situation was found for the cryomilled sample. It undergoes liquid−crystal transition very easily. However, when both samples were stored at 298 K under dry conditions (humidity equal to 10%), the recrystallization process was not detected for a long time in both samples. The X-ray diffractogram measured after 210 days still had the broad halo characteristic for the glassy material.

Finally, using BDS and DSC techniques, we analyzed the properties of the sample obtained after heating and cooling of cryomilled GCM. A DSC scan obtained during the reheating of a previously melted and quenched cryomilled GCM sample is shown as a blue line in Figure 15. As can be seen, the characteristic signature for T_g in the heat flow is observed at the same temperature as in the case during the initial heating of that cryomilled sample ($T_g = 338$ K). The same procedure of heating and cooling of the milled GCM was applied in the case of BDS measurement. To compare both the position and the shape of the α-relaxation peak, the milled GCM was first heated to its melting point. Thereafter, it was kept at 440 K for 5 min to ensure that it was completely molten. In a subsequent step, the spectrum of the sample was recorded at a temperature of 393.15 K. The positions and shapes of the structural relaxation peaks were exactly the same in both cases. Thus, it is clear that the melting of the ground sample results in the same relaxation and thermodynamical transformations as those observed for the quenched sample.

Conclusions

From our studies of the amorphous GCM drug we can draw the following conclusions:

1. Quench-cooling of the melt as well as cryogenic grinding can be successfully used to achieve the glassy GCM drug. It was shown that none of the examined amorphous samples underwent any chemical degradation. Thus, the thermal decomposition as suggested in the literature does not occur. Moreover, the sample is stable during the time required for its complete melting. Some signs of degradation were detected only after 60 min of heating at the melting temperature. Therefore, one can conclude that either of the described methods of amorphization may be used to obtain the glassy GCM material.

2. We have determined that milling under cryogenic conditions as well as quench-cooling leads to structural changes in the GCM molecule. It was shown that conversion to the glassy state or dissolution of the examined drug leads to an amide−imidic acid tautomerism. Moreover, the UPLC result indicated that there is more than one possible imidic acid form in the glassy state.

3. Using BDS spectroscopy, we have studied the dielectric properties of GCM in liquid and glassy states. We have provided an almost complete characterization of the molecular mobility of the quenched and cryomilled samples. In both cases, the structural relaxation exhibits two secondary modes. The temperature dependence of the α-relaxation times measured for quenched GCM over the 10 decades can be satisfactorily described singly with the VFT law. The values of T_g determined for quenched GCM and milled GCM from VFT fits are equal to 338.98 and 342.15 K, respectively. Moreover these values are in good agreement with those obtained from DSC measurements. The high values of T_g indicate the possibility to prepare amorphous GCM that is completely stable at room temperature, and also at the human body temperature.

4. DSC and BDS techniques have also shown that both of the investigated systems exhibit opposite tendencies to crystallization in nonisothermal conditions. While the quenched GCM sample is stable in a wide temperature range, the cryomilled GCM crystallizes very easily. However, during the storage of samples under dry conditions at room temperature, any sign of crystallization was not observed even after 210 days. Moreover, in the dielectric loss spectra of the milled product at temperatures above 373 K, one can observe an additional relaxation peak which was not observed during measurements of the quenched GCM. Its occurrence is probably connected with the crystallization process observed at this temperature. However, this new relaxation process vanished after heating the sample to the melting point.

Acknowledgment. The authors Z.W., K.G., M.P., K.K., and K.A. are deeply thankful for the financial support of their research within the framework of the project entitled *From Study of Molecular Dynamics in Amorphous Medicines at Ambient and Elevated Pressure to Novel Applications in Pharmacy* (Contract No. TEAM/2008-1/6), which is operated within the Foundation for Polish Science Team Programme cofinanced by the EU European Regional Development Fund. Moreover, K.G. and K.K. thank FNP for awarding grants within the framework of the START Programme (2009). The authors are deeply grateful to Doctor Manoj Kolel-Veetil (Chemistry Division, Material Science & Technology Division and SAIC, Naval Research Laboratory in Washington) for helpful discussions and valuable advice.

MP100077C